Sheffield Hallam University

Role of precombustion chamber design in feed-system coupled instabilities of hybrid rockets

LEE, J, BERTOLDI, AEDM, ANDRIANOV, A, BORGES, RA, VERAS, CAG, BATTISTINI, Simone, MORITA, T and HENDRICK, P

Available from Sheffield Hallam University Research Archive (SHURA) at:

http://shura.shu.ac.uk/27601/

This document is the author deposited version. You are advised to consult the publisher's version if you wish to cite from it.

Published version

LEE, J, BERTOLDI, AEDM, ANDRIANOV, A, BORGES, RA, VERAS, CAG, BATTISTINI, Simone, MORITA, T and HENDRICK, P (2020). Role of precombustion chamber design in feed-system coupled instabilities of hybrid rockets. Journal of Propulsion and Power, 36 (6), 796-805.

Copyright and re-use policy

See http://shura.shu.ac.uk/information.html

Sheffield Hallam University Research Archive
http://shura.shu.ac.uk

The role of pre-combustion chamber design in the feed-system coupled instability of hybrid rockets

Jungpyo Lee[1,*], Artur Elias De Morais Bertoldi[2], Artem Andrianov[3], Renato Alves Borges[4], Carlos Alberto Gurgel Veras[5]
University of Brasilia, Brasilia, Federal District, 70910-900, Brazil

Simone Battistini[6]
Sheffield Hallam University, Sheffield, S1 1WB, United Kingdom

Takakazu Morita[7]
Tokai University, Hiratsuka, Kanagawa, 259-1292, Japan

and
Patrick HENDRICK[8]
Free University of Brussels, Brussels, 1050, Belgium

Oxidizer feed-system coupled instabilities have been observed in several liquid and hybrid propellant rocket engines, though, not likely to be catastrophic for the latter. However, severe pressure oscillation in hybrid rocket may result in a significant reduction in the performance of the propulsion system restricting the application of the technology. In this research, it was studied, theoretically and experimentally, feed-system coupled instabilities for hybrid rocket engines. Two test campaigns were performed to investigate the effects of the pre-combustion chamber and oxidizer injector configurations on engine pressure oscillation. Then, an extended mathematical formulation, including the injector pressure drop, the pre-combustion chamber residence time, the gas residence time, and the combustion time lag, has been proposed. The investigation was based on a transfer function using the stability limit analysis and the root locus method. It has been found that the configuration of pre-combustion chamber plays an important role in the nature of the feed-

[1] Professor, Aerospace Engineering, *Corresponding Author : jungpyo_lee@aerospace.unb.br
[2] Professor, Aerospace Engineering.
[3] Professor, Aerospace Engineering.
[4] Professor, Department of Electrical Engineering.
[5] Professor, Department of Mechanical Engineering.
[6] Senior Lecturer, Department of Engineering and Mathematics.
[7] Professor, Department of Aeronautics and Astronautics.
[8] Professor, Department Aero-Thermo-Mechanics.

system coupled instabilities, and a correlation was proposed to predict the fundamental frequency based on the oxidizer pre-combustion chamber residence time. The work has shown that the pre-combustion chamber length and the oxidizer injection velocity are key parameters that affect the period of the pressure oscillations in hybrid engines subjected to feed-system coupled instabilities.

Nomenclature

$A_{n.t}$ = nozzle throat area (m^2)

a, n = regression rate constants

c^* = characteristic velocity (m/s)

c' = combustion time lag coefficient

D = fuel port diameter (mm)

f = frequency (Hz)

G = oxidizer mass flux ($kg/m^2/s$)

g_c = constant of proportionality; for SI: (1 $kg \cdot m/N/s^2$), for EE: (386.087 $lb_m \cdot in/lb_f/s^2$)

L_{pre} = pre-combustion chamber length (mm)

L_f = fuel length (mm)

L^* = L-star (m)

M = Mach number

M_c = chamber gas mass

$\dot{m}$ = mass flow rate (kg/s)

O/F = oxidizer to fuel mixture ratio

P = pressure (bar)

P' = pressure oscillation amplitude

P^* = $P'/\overline{P_c}$

ΔP = injector pressure drop

ΔP^* = $\frac{2\Delta P}{\overline{P_c}}$

R = gas constant, 8.314 J/mol/K

$\dot{r}$ = regression rate (mm/s)

T = temperature (K)

u = velocity (m/s)

V_c = chamber volume (m^3)

Greek Symbols

γ = specific heat ratio

η_c = combustion efficiency

θ_g = ~~bulk~~ gas residence time (s)

ρ = density (kg/m^3)

τ_{comb} = combustion time lag (ms)

τ_{pre} = pre-combustion chamber residence time (ms)

ω = angular frequency (rad/s)

Superscripts

$\bar{\cdot}$ = average

$\hat{\cdot}$ = Laplace transform variable

Subscripts

c = combustion gas, chamber

f = fuel

i = injector

ini = initial

ox = oxidizer

pre = pre-combustion chamber

t = oxidizer tank

th = theoretical

tot = total

I. Introduction

Combustion instabilities in rocket systems produce undesirable pressure oscillations in the combustor. The phenomena occur when the fluid and the combustion dynamics of the system result in sustained oscillatory energy affecting the combustion process itself, the liquid propellant supply, and the structural integrity of the motor [1]. Combustion instabilities cause gas pressure peaks and increase the heat transfer to the combustor walls to such an extent that may destroy the whole system. Hybrid rocket pressure oscillations of low frequency and large amplitude have been observed by many researchers [2-7]. Such manifestation is not as catastrophic for hybrid rocket engines as it is for liquid and solid systems. However, severe pressure oscillation can result in a significant reduction in the performance of the propulsion system, trigger other types of instabilities [2], or restrict the application of the technology, depending on mission requirements. Some studies have confirmed the influence of the pre-combustion chamber flow condition on the stability of hybrid rocket engines. It is generally accepted that the stability level of the motor is controlled by some features of the pre-combustion chamber, like the injector configuration, the chamber volume/geometry, and the oxidizer gas heating sources. It is known that the type of liquid oxidizer injection has a great influence on the combustion instability of hybrid rocket engines [8-13]. However, the extent of the impact of the injection system on motor stability differs. For instance, Boardman et al. [8, 9] have shown that the axial injectors enhanced combustion stability as compared to the radial and the 45-deg configurations. Pucci [10] and Carmicino [11] have obtained similar results, i.e., axial injectors are more efficient in stabilizing the gas pressure than radial and swirl oxidizer injectors. They claimed that a strong central toroidal recirculation zone (CTRZ) in the pre-combustion chamber entrains hot combustion gases and cold oxidizer, and the hot-gas recirculation zone heats the incoming oxidizer to a sufficiently high temperature to decompose fuel ahead of the flame leading edge, thus it can stabilize the flame sheet. Additionally, Bellomo et al. [12] and Kim et al. [13] have shown that the swirl injectors enhance combustion stability more efficiently than the axial counterpart. They concluded that low-frequency instability could be suppressed by the application of swirl injectors. In spite of the strong influence of the injection system on the instability of hybrid rocket engines, it seems premature to affirm that it is the sole parameter to be concerned about. Preliminary studies from our research group have indicated a significant influence of the pre-combustion chamber design containing injector on the feed-system coupled instability of hybrid rocket engines. Therefore, a deeper investigation on the effects of pre-combustion chamber configuration on the low-frequency instabilities in hybrid rocket systems is opportune.

Feed-system coupled instabilities have been observed in hybrid and liquid rocket engines. It is a type of dynamic instability in which the time-dependent response of the propellant flow is related to the unsteady combustion pressure. Feed-system coupled instabilities in the context of liquid rocket engines are well understood, and correlations to predict the fundamental frequency of the instability have been developed [14, 15]. However, it is not recommended to directly apply the instability theory of liquid rocket engines to its hybrid counterpart. Hybrid rocket combustion characteristics differ from those of liquid engines in many aspects in spite of the similarities related to the oxidizer feed-system response to pressure oscillation inside the combustor.

This paper presents a new approach to predict feed-system coupled instabilities of hybrid rockets engines. The proposed method takes into account the influence of the parameters such as the pre-combustion chamber residence time, the ~~bulk~~ gas residence time, the injector pressure drop, and the combustion time lag on the combustion instabilities of hybrid rocket engines. For that, a linear analysis of the stability condition using the root locus tool from linear systems theory was conducted. Furthermore, the sensitivity of the system to the variation of some design parameters of the engine was analyzed. The proposed model was validated using experimental data which were also employed to infer a correlation to predict the fundamental frequency of the system as a function of the pre-combustion chamber residence time. The paper is organized as follows: first a linearized model for hybrid rocket engine instabilities is presented (i); followed by the application of the proposed model on stability limit and root locus analysis (ii); then, we describe the experimental setups and the associated data obtained from two test campaigns (iii) that were employed to validate the proposed model (iv); and a correlation to predict the fundamental frequency as a function of the oxidizer pre-combustion chamber residence time has been proposed (v).

II. Linearized Model for Hybrid Rocket Engine Instabilities

The Time-Lag-Based combustion instability model has been proposed to explain the low-frequency instabilities in hybrid rocket engines. The basis of the hypothesis is that a time lag exists between an arbitrary fluctuation in the propellant flow and its subsequent manifestation in the combustion chamber pressure [16, 17]. The time lag concept in hybrid rocket engines accounts for the delay associated with the evolution of combustion gases in relation to the time the oxidizer had been injected.

Instabilities that are commonly generated in hybrid rocket engines are bulk mode, meaning that pressure oscillation can occur over the entire volume of the combustion chamber. Hybrid rocket combustion chamber pressure depends on the rate of gaseous oxidizer mass inflowing into the flame over fuel grain surface, the fuel mass

evaporated from the solid fuel surface, the propellant mass expelled through a nozzle, and the accumulation of the gas in the chamber [18]. The continuity equation which is a bulk mass balance in a hybrid rocket combustion chamber can be written as

$$\frac{d}{dt}\left(\rho_c V_c\right) = \dot{m}_{ox}\left(t\right) + \dot{m}_f\left(t\right) - \dot{m}_n\left(t\right) \tag{1}$$

The present research is focused on the feed-system coupled instability, not on the intrinsic low frequency oscillations where feed-system dynamics is very rigid. A certain residence time, τ_{pre}, is required before the oxidizer flowing through the injector reacts in the flame with the fuel evaporated from the solid grain surface. The proposed residence time refers to the time delay that the oxidizer flow leaves the injector and reaches the flame zone. Hence, the oxidizer entering the flame zone at time (t) corresponds to the oxidizer leaving the injector at time (t- τ_{pre}). It is an approximation of complex intermediate processes, accounting for the oxidizer impingement, the atomization, the evaporation, and the flow towards the flame zone before the oxidizer is mixed with the fuel vaporized from the grain. The time delay describes the evolution of these processes and, for simplicity, it was replaced by two distinct events as shown in Eq. (2).

$$\dot{m}_{ox}\left(t\right) = \dot{m}_i\left(t - \tau_{pre}\right) \tag{2}$$

The oxidizer passing through an injector orifice, with cross-sectional area A_i and discharge coefficient C_d, satisfies the Bernoulli's equation, with a mass flow rate given by:

$$\dot{m}_i = C_d A_i \sqrt{2\rho_{ox}\left(P_t - P_c\right)} \tag{3}$$

The oxidizer mass flow rate has a strong influence on the regression rate of the solid fuel in hybrid rocket combustion, and the fuel burning-rate, $\dot{m}_f\left(t\right)$ in Eq. (1), can be expressed as:

$$\dot{m}_f(t) = \rho_f \pi L_f D(t) \dot{r}(t) = \rho_f \pi L_f D(t) a G^n(t) = \rho_f \pi L_f D(t) a \left(\frac{\dot{m}_{ox}(t - \tau_{comb})}{\frac{\pi}{4} D^2(t)} \right)^n \tag{4}$$

$$\dot{r}(t) = f_n\left(\dot{m}_{ox}(t - \tau_{comb})\right) = f_n\left(\dot{m}_i(t - \tau_{pre} - \tau_{comb})\right) \tag{5}$$

Besides τ_{pre}, another time delay τ_{comb} was also considered in this research. Although both parameters represent time lags, τ_{comb} has a different physical meaning from τ_{pre}. The former is referred to as the time necessary for the fuel mass flow rate to adjust to change in the oxidizer mass flow rate into the flame. Hence, the oxidizer existing in the flame zone at some time (t-τ_{comb}) is consumed to produce vaporized fuel on the solid surface at a later time (t). It is an approximation of complex intermediate processes, and the time line of the events occurred during the combustion time lag are: heat is transferred from the flame to the surface of the fuel (i), then, it melts (ii) and vaporizes the fuel (iii). Gaseous fuel is transported (iv) and reacts with the oxidizer in the flame zone (v).

The last term in Eq. (1), $\dot{m}_n(t)$, is the mass flow rate of combustion products at the nozzle entrance. From compressible isentropic flow, the mass ejection rate is given by Eq. (6), which can be expanded in a Taylor series using pressure and temperature parameters, normalized by the mean flow rate gas state [17]. The quasi-steady linearization of this term is expressed by Eq. (7) in terms of the normalized states ($\overline{\dot{m}}, \overline{P}, \overline{T}$) and the perturbative parts ($\dot{m}_n'$, P', T'). The chamber pressure, P_c, can be decomposed into steady ($\overline{P}_c$) and fluctuating (P_c') components of the property. Accordingly, other parameters such as the mass flow rate, the temperature, the density, and the chamber volume can be decomposed into steady and fluctuating parts.

$$\dot{m}_n = \frac{p_{tot}}{\sqrt{T_{tot}}} \mathrm{A}_{n.t} M \sqrt{\frac{g_c \gamma}{R} \left(1 + \frac{\gamma - 1}{2} M^2\right)^{\frac{\gamma+1}{\gamma-1}}} \tag{6}$$

$$\frac{\dot{m}_n'}{\overline{\dot{m}}} = \frac{p_c'}{\overline{p_c}} - \frac{1}{2} \frac{T_c'}{\overline{T_c}} \tag{7}$$

For simplicity, propellant gas in a chamber obeys the perfect gas law, subjected to the isentropic process, that is

$$P_c \rho_c^{-\gamma} = const \tag{8}$$

From the linearization and the Laplace transforms of the perturbation equations Eq. (1) and Eq. (3), after substituting Eq. (2), Eq. (4), Eq. (7), Eq. (8), and the ideal gas law equation into Eq. (1), we can obtain a transfer function for low-frequency combustion instabilities in hybrid rocket engines expressed by the following equation included the time delays τ_{pre} and τ_{comb}.

$$\frac{\hat{p}_c^*}{\hat{p}_t^*} = \frac{\dfrac{O/F}{O/F+1} + \dfrac{n}{O/F+1} exp^{-\tau_{comb}S}}{\dfrac{2\Delta P}{\overline{P_c}}\left(\dfrac{\theta_g}{\gamma}S + \dfrac{\gamma+1}{2\gamma}\right)exp^{\tau_{pre}S} + \left(\dfrac{O/F}{O/F+1} + \dfrac{n}{O/F+1} exp^{-\tau_{comb}S}\right)} \tag{9}$$

In order to derive Eq. (9), the mass flux exponent in Eq. (4) was considered equal to 0.5 (n=0.5). This is a reasonable assumption since the oxidizer mass flux exponent has been observed to range from 0.5 to 0.75 regardless of the type of propellant for most hybrid propulsion systems [1, 19, 20]. And the time rate of change of the chamber gas volume was neglected because the fuel regression rate is on the order of a few mm/s, much slower than combustion time scales.

The term θ_g in Eq. (9) referred to the gas residence time, which is the average time that a gas element resides in the chamber prior to reaching the nozzle entrance, was written in terms of the rocket engine parameters as follows [18, 21]

$$\theta_g = \frac{\overline{M}_c}{\overline{\dot{m}}_n} = \frac{\overline{\eta}_c \overline{c_{th}^*}}{A_t g_c}\left(\frac{\mathrm{V}}{R\overline{T}}\right)_c \tag{10}$$

Pre-combustion chamber residence time (τ_{pre}) is modeled as shown in Eq. (11). It takes into account the combined elapsed time for the oxidizer to break up into small particles (atomization) and the time for the droplets to evaporate and reach the flame front. In that sense, the type of oxidizer, the design of the injector, the size of the pre-

chamber, and the interaction between the droplets and the bulk flow play an important role in the parameter. Eq. (11) states that these phenomena occur in the time when the oxidizer flow travels from the exit of the injector plate to the flame front in the boundary layer.

$$\tau_{pre} = \frac{L_{pre}}{u_{pre}} \tag{11}$$

Similarly, the combustion time lag (τ_{comb}) is modeled by the following equation

$$\tau_{comb} = \mathrm{c}' \frac{L_f / 2}{u_f} \tag{12}$$

where τ_{comb} is physically similar to the boundary-layer lag (τ_{bl}) proposed by Karabeyoglu et al. [22], corresponding to the time necessary for the hybrid boundary layer properties to adjust to change in the oxidizer mass flow flux. The model of the boundary-layer delay was suggested considering an incompressible turbulent boundary layer without blowing effects and chemical reactions, and τ_{bl} is proportional to the time of flight of a fluid particle from the leading edge of the boundary layer to the specific axial location at the speed of the freestream flow (τ_{comb} was modeled in the same way). The coefficient c' in Eq. (12) can be determined empirically, and it should be estimated for the specific operating conditions. The value was estimated to be approximately 2.05 for typical hybrid rocket operation by Karabeyoglu et al. [22].

III. Combustion Stability Analysis

A. Stability Limit Analysis

Stability investigations can be performed with the derived transfer function. Stability limit approach is useful to investigate stability behavior of a rocket engine by altering various motor operating parameters [23]. In order to analyze the stability limit, the denominator in the characteristic equation of the system in Eq. (9) was set to zero, leading to Eq. (13) after substituting $s=i\omega$. The stability limit analysis splits the state space into two regions, nominally stable and unstable.

$$\frac{2\Delta P}{\overline{P_c}}\left(\frac{\theta_g}{\gamma}i\omega+\frac{\gamma+1}{2\gamma}\right)exp^{\tau_{pre}i\omega}+\left(\frac{O/F}{O/F+1}+\frac{n}{O/F+1}exp^{-\tau_{comb}i\omega}\right)=0 \tag{13}$$

Using the Euler's formula for complex exponential functions, the denominator can be written in terms of real and imaginary parts. The real and the imaginary parts of the denominator give, respectively, the following equations:

$$\Delta P^*\frac{O/F+1}{\gamma}=\frac{O/F+n\cos\left(\omega^*_{comb}\right)}{\sqrt{\left(\frac{\gamma+1}{2}\right)^2+\left(\frac{\theta_g}{\tau_{pre}}\omega^*_{pre}\right)^2-\left(\frac{n\sin\left(\omega^*_{comb}\right)}{\Delta P^*\left(\frac{O/F+1}{\gamma}\right)}\right)^2}} \tag{14}$$

$$\Delta P^*\frac{O/F+1}{\gamma}\left\{\frac{\theta_g}{\tau_{pre}}\omega^*_{pre}\cos\left(\omega^*_{pre}\right)+\frac{\gamma+1}{2}\sin\left(\omega^*_{pre}\right)\right\}-n\sin\left(\omega^*_{comb}\right)=0 \tag{15}$$

where $\Delta P^*=\frac{2\Delta P}{\overline{P_c}}$, $\omega^*_{pre}=\omega\tau_{pre}$, and $\omega^*_{comb}=\omega\tau_{comb}$.

By solving Eq. (14) and Eq. (15), it can be found that ΔP^* is a function of θ_g/τ_{pre} and ω^*_{comb}. The relation among ΔP^*, θ_g/τ_{pre}, and ω^*_{comb} is represented in Fig. 1. Stability limit curves were plotted specifically for $\gamma = 1.27$, O/F = 3, and three arbitrary values of ω^*_{comb}, $\pi/4+2\pi(z-1)$, $5\pi/6+2\pi(z-1)$, and $5\pi/4+2\pi(z-1)$, where z is an integer. For each ω^*_{comb} value, the region of stable operation is above the limit curve. It can be seen that the stable combustion regime becomes broad as θ_g/τ_{pre} increases at a fixed ΔP^*, or as ΔP^* increases at a fixed θ_g/τ_{pre}. It could be also confirmed from the plot that the stable regime is greatly influenced by ω^*_{comb}. There are several strategies to improve feed-system coupled stability, e.g., by increasing the pressure difference between the feed line and the combustion chamber, by increasing the volume of the combustion chamber (increased θ_g), or by reducing the pre-combustion chamber length or the cross-sectional area of injector orifices (reduced τ_{pre}).

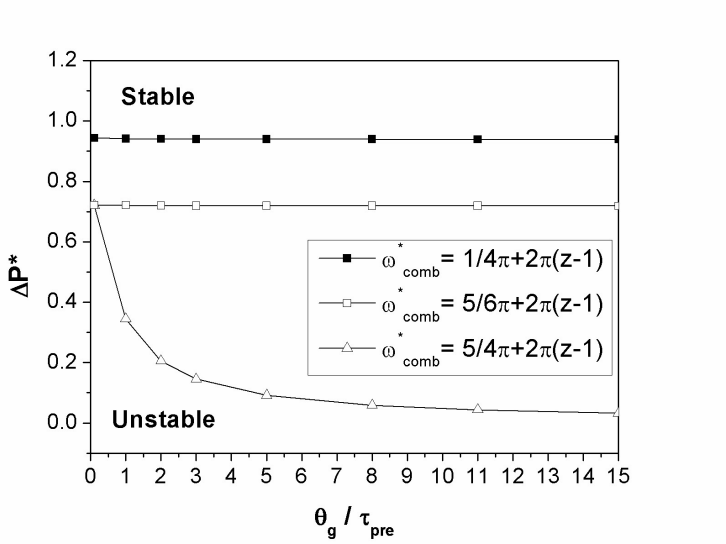

Fig. 1 Stability limit for feed-system coupled instability in hybrid rockets.

B. Root Locus Analysis

Another tool that can be used to investigate the stability of the system is the root locus. This is a representation of how the roots of a system change on the complex plane after varying a certain parameter. Its primary advantage lies in the fact that the gain and phase of the system are presented simultaneously. The root locus can be used to calculate the neutral oscillation frequency (NOF, also called Peak Oscillation Frequency) for different values of τ_{pre} and τ_{comb}. This is the corresponding frequency at which the locus crosses the imaginary axes of the complex plane causing instability in the system. Parametric analysis with the root locus is easier to perform than that using the condition in Eq. (14) and Eq. (15), because different values of the parameters can be evaluated, simultaneously, on a single plot of the root locus. The transfer function, Eq. (9), can be adjusted to draw the root locus using the Padé approximant for the two exponential terms at the denominator. The resulting transfer function is a numerical approximation of Eq. (9). Fig. 2 shows the root locus obtained with this approximation. The instability is caused by the two low-frequencies, complex poles close to the origin of the complex plane. The two loci departing from these two poles cross the instability boundary for a gain of 3.63 at a frequency of 732 rad/s, making the system unstable. The gain is the numerical value that expresses the parametric variation of the transfer function. This means that the gain changes with the variation of the parameters. By repeating the analyses with different values of τ_{pre} and τ_{comb} allows to emphasize the relationship between the natural frequency and these parameters.

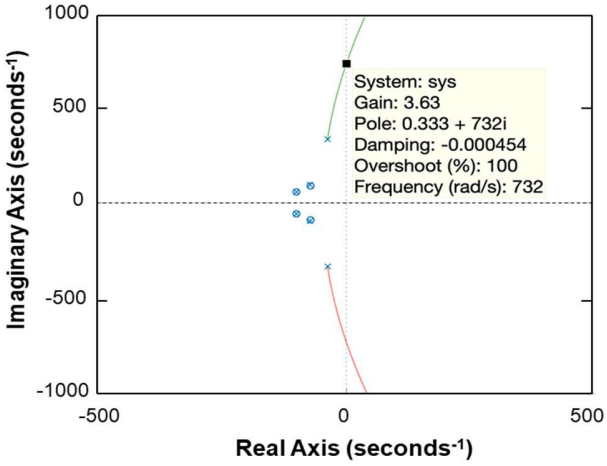

Fig. 2 Root locus result.

B.1 Parametric Analysis Result

A system parametric analysis was conducted using the root locus method to find out how the parameters in the transfer function, Eq. (9), affect the frequency. Fig. 3 shows the frequency of the system as a function of τ_{pre} for different values of τ_{comb}. For the analysis, the parameters O/F=3, n=0.5, $\overline{P_c}$ =38.5 bar, ΔP=18.6 bar, θ_g=0.0266 sec, and γ=1.27 were held constant. It can be seen that the fundamental frequency has a strong negative correlation with τ_{pre}, especially, when it is small value. Decreased pre-combustion chamber residence time causes higher system frequency response, regardless of the combustion time lag. The influence of τ_{comb} on the frequency of the system is also clear, mostly for small values of τ_{pre}. The relative influence of the combustion time lag on the frequency response of the system, for different values of τ_{pre}, can be examined with the help of Fig. 4. For pre-combustion chamber residence times greater than 0.1 s, the combustion time lag shows little influence on the fundamental frequency of the system, ultimately defined by τ_{pre}. It should be noticed that θ_g and O/F ratio also play their role on the fundamental frequency of the system, as shown in Fig. 5. However, in all of our predictions, the influence of τ_{pre} on the primary oscillation frequency surpassed that of any other parameter.

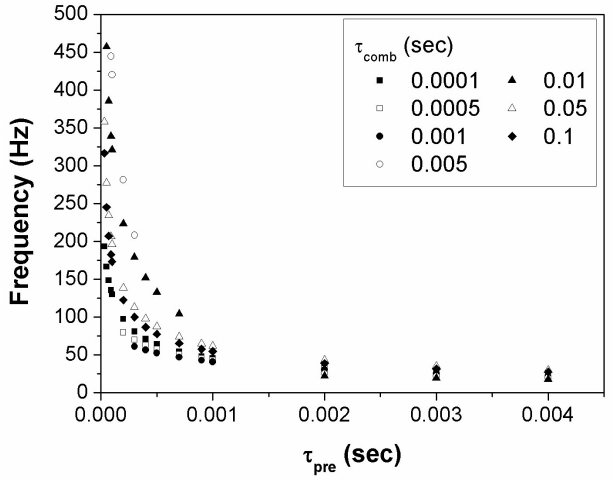

Fig. 3 Effect of τ_{pre} on fundamental frequency with different values of τ_{comb}.

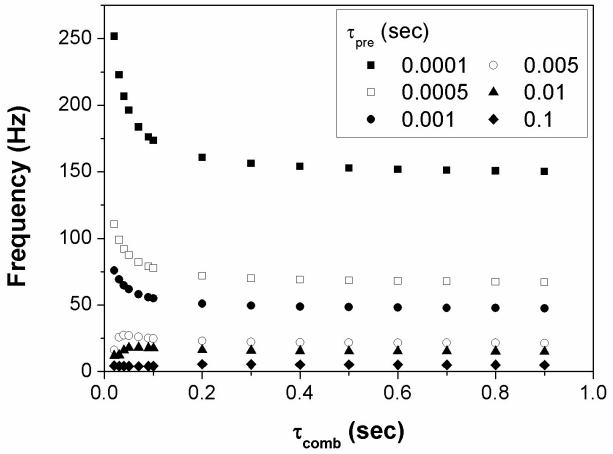

Fig. 4 Effect of τ_{comb} on fundamental frequency with different values of τ_{pre}.

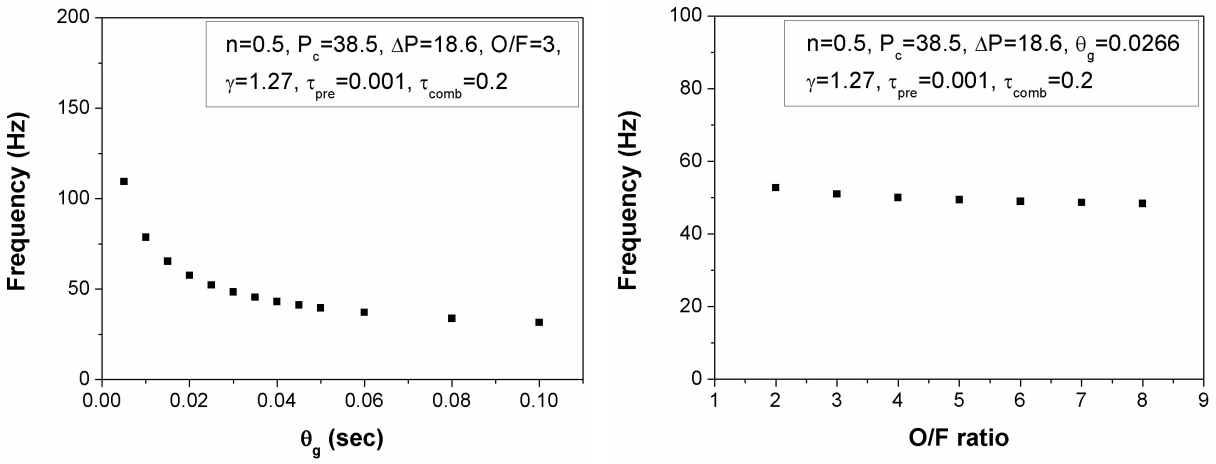

(a) (b)

Fig. 5 Effect of θ_g (a) and O/F (b) on fundamental frequency.

IV. Experimental Setup

It is widely known that parameters such as the pressure drop, the gas residence time in the combustion chamber, and the vaporization time lag have strong influence on the feed-system coupled instability of liquid-fed rocket engines [14]. These parameters have also a great impact on the stability limits of hybrid rocket engines. This study, however, focuses on the influence of the pre-combustion chamber configuration included an injector on the instability of the system and on the characteristics of the oscillation frequency of the combustion chamber. Therefore, it relies on experimental data to validate the proposed extended model.

Data from two test campaigns, one at the Universidade de Brasília (UnB, Brazil) and the other at the Université Libre de Bruxelles (ULB, Belgium), helped investigate the feed-system coupled instability of hybrid rockets. ~~validate the proposed model~~ For the experiments, the laboratories employed different combustion chamber setups. Nevertheless, the hybrid propulsion systems were somehow similar in size, operating pressure, and oxidizer mass flow rate. The test bench setups were composed of a hybrid rocket combustion chamber with temperature and pressure transducers, an oxidizer feed system, an ignition device, and a data acquisition (DAQ) system. Combustion chamber pressure oscillations were measured by piezoelectric dynamic pressure transducers, a Kistler 6052C at the UnB test bench and a Kistler 6061B at the ULB test bench. Strain type pressure transducers were installed into the combustion chamber and the oxidizer feeding line for static pressure measurements. The analog signals coming from the transducers were sampled at frequency of 5~10 kHz, digitally converted (16 bit resolution), processed, and recorded by a NI PCIe-6320 data acquisition card system (UnB). For the ULB test bench, the signal processing was performed by a NI USB-6218 board and a NI USB-9215 card system. Firing tests were performed automatically with the help of logic controllers programed in a LabVIEW environment.

Table 1 shows the main characteristics of the two test benches and the specifications for the firing tests conducted at each university. Liquid nitrous oxide (N_2O) was chosen as the oxidizer in combination with two different fuels, paraffin and high density polyethylene (HDPE). The schematic drawings for the UnB and the ULB test motors are shown in Fig. 6, respectively. The pre-combustion chamber of the UnB motor is exchangeable, allowing motor configurations with different chamber lengths. A detailed description of the system can be found in [24, 25].

Table 1 Specification of combustion tests

	Universidade de Brasília (UnB)	Université libre de Bruxelles (ULB)
Oxidizer	Liquid N_2O	Liquid N_2O
Solid Fuel	Paraffin, HDPE	Paraffin
Fuel Length	101 mm (Paraffin), 207 mm (HDPE)	107.5 mm
Fuel Port Diameter	51, 34 mm	30 mm
Pre-combustion Chamber Length	56.6, 76.6, 157.6, 177.6 mm	102.5 mm
Pre-combustion Chamber Diameter	120 mm	99 & 130 mm
Injector Type	One-hole Axial, SH[a]	SH[a], HC[b], PSW[c], VOR[d]
Oxidizer Mass Flow Rate Range	0.21-0.56 kg/s	0.35-0.65 kg/s
Oxidizer Tank Pressure	50-70 bar	60-80 bar
Chamber Pressure Range	3-43 bar	16-30 bar

[a]Showerhead Type, [b]Hollow Cone Type, [c]Pressure Swirl Atomize Type, [d]Vortex Type

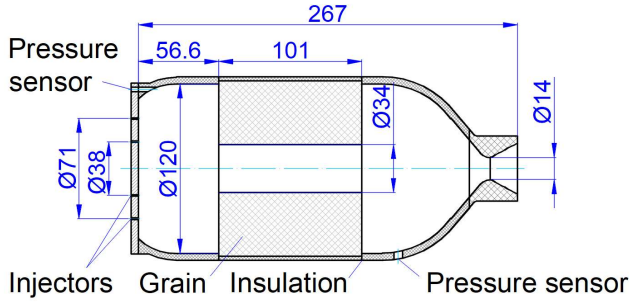

(a)

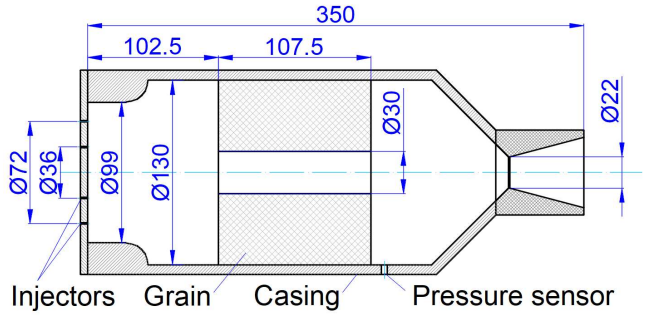

(b)

Fig. 6 Schematic drawings of UnB motor(a) and ULB motor(b)

Previous researches have pointed out the strong influence of the oxidizer injection type on the instability of hybrid rockets engines [8-13]. For instance, there are studies [12, 13] claiming that swirl injectors increased the stability of hybrid rocket engines, over axial injectors, while others [8-11] have reported contradictory results. Therefore, the test campaign at ULB was used to verify the effects of oxidizer injection system on the motor`s stability. In total, five oxidizer injection systems were tested, as shown in Table 2. The recirculation zone, formed in the pre-combustion chamber, plays an important role in the stability of the system. Thus, a 15° injection angle hollow-cone (HC) injector was designed to generate a large ring vortex at the head end of the fuel grain. The pressure swirl (PSW) injector plate had six individual pressure-swirl injectors, each having four tangential ports to generate the rotational flow. Vortex injectors have been applied in hybrid rocket engines aiming to increase the fuel regression rate. Their behavior regarding combustion instabilities has been also object of investigation. The vortex injector from ULB was comprised of six holes (3 mm diameter) displayed radially along the plate with a 45° degree injection angle [26]. Another showerhead injector of the UnB motor was designed with holes equally distributed in two concentric radii with six, 1.0 mm diameter, orifices along the inner circumference and ten, 2.0 mm diameter orifices, in the outer circumference.

The test campaign conducted by UnB had the main objectives of verifying the influence of pressure drop between the feeding line and the combustion chamber (i); the injection oxidizer flow velocity (ii); and the pre-combustion chamber length (iii) on the stability level of the motor; and analyzing the fundamental frequency (iv).

Table 2 Main parameters of used injectors

Injector Type		Hole Diameter (mm) / Number of holes	Inclined angle to axial axis	Injector L/D
One-hole Axial	UnB	10.25/1	0 º	3
Showerhead	UnB	Case 1) 2/16 Case 2) 1/6 & 2/10	0 º	4 4 & 8
	ULB	Case 1) 1.4/11 Case 2) 1.4/21	0 º	5.4
Hollow Cone	ULB	1.4/11	15º	
Pressure Swirl Atomizer	ULB	1.5/9	0 º	
Vortex	ULB	3/6	45º	

V. Results and Discussions

Data from the firing tests along with some calculated parameters are given in Table 3. Paraffin was selected as the fuel for tests #1 to #26, and HDPE for test #27. The pre-combustion chamber length, L_{pre}, was calculated as the distance from the injector exit to the head end of the fuel grain. ΔP is the injector pressure drop measured as the difference between the feed line pressure near the oxidizer tank and the combustion chamber pressure at the beginning of the combustion. The parameter P'_{max} / P_c is the maximum chamber pressure oscillation amplitude divided by the initial chamber pressure. Recorded samples of the chamber pressure and the feed line pressure were taken as the reference value for the instability analysis. In hybrid rockets, the combustion port increases as the solid fuel is radially consumed. The fuel length can also be altered if no component is installed to inhibit axial combustion at both ends of the fuel. In the models, Eq. (11) and (12), the port diameter and the fuel length are the key parameters to calculate τ_{pre} and τ_{comb}. Unfortunately, real-time observation of the port diameter and the fuel length was not carried out in this research, giving complexity to perform such measurements. Therefore, for the analysis, the initial values for most of the experimental parameters were adopted. The initial geometry of the combustion chamber was based on the initial fuel port diameter and length, in addition to the initial volumes of the combustion chamber and the pre-combustion chamber. The initial fundamental frequency, f_{ini}, of the pressure oscillation was taken as that at the onset of the combustion instabilities. The initial frequency was chosen after applying the short-time Fourier Transform to data whose amplitude pressure oscillation were 5% higher than the chamber pressure. Therefore, f_{ini} values for the stable test cases were disregarded (Tests #1, #3-4, #14, #16-26) in Table 3. To calculate τ_{pre} and τ_{comb}, Eq. (11) and Eq. (12) were used, respectively. Flow velocity in the pre-combustion chamber, u_{pre}, in Eq. (11), was taken as the mean value between the velocity at the injector exit and the velocity at the head end of fuel grain. The nitrous oxide injected in the pre-combustion chamber was assumed to be half in liquid phase and half in the gas phase. The quality parameter χ was then set to 0.5, and it was used to calculate the flow velocity at the injector exit. Flow in the fuel port was considered an ideal gas. The value of the coefficient c' in Eq. (12) should be estimated for the specific operating conditions of a given hybrid rocket engine. A rigorous estimation of c' is beyond the scope of this work, and, for simplicity, a constant value of 1.0 for c' is considered in this analysis. The proposed value is smaller than the one (c'=2.05) used in the τ_{bl} model in [22], but it is larger than that (c'=0.55) obtained considering a boundary layer with frozen chemistry and without blowing effect [22].

Table 3 Hybrid combustion instability test results

Test No.		Injector type	L_{pre} (mm)	D_{ini} (mm)	O/F	P_c (bar)	ΔP (bar)	τ_{pre} (ms)	τ_{comb} (ms)	θ_g (ms)	P'_{max} / P_c (%)	f_{ini} (Hz)
1	UnB	SH 2/16	56.6	51	1.7	13.5	37.5	2.20	0.73	13.62	0.2	-
2	UnB	SH 2/16	56.6	34	6.5	44.0	14.5	0.53	0.28	12.33	7.8	156
3	UnB	SH 1/6+2/10	56.6	34	2.8	25.6	19.1	1.06	0.48	14.99	1	-
4	UnB	SH 1/6+2/10	56.6	34	4.9	3.5	35.5	0.08	0.03	1.75	3	-
5	UnB	SH 1/6+2/10	56.6	34	4.2	37.0	13.3	0.69	0.36	8.68	5.5	140
6	UnB	SH 1/6+2/10	56.6	34	4.2	40.5	10.5	0.76	0.41	26.42	6.2	166
7	UnB	SH 1/6+2/10	56.6	34	3	39.5	8.8	0.93	0.49	24.56	5.6	150
8	UnB	SH 1/6+2/10	56.6	34	5.5	39.9	10.6	0.58	0.33	7.89	5.4	145
9	UnB	SH 1/6+2/10	56.6	34	5.1	37.0	11.2	0.64	0.34	15.89	5.9	133
10	UnB	SH 1/6+2/10	56.6	34	5.1	36.5	8.5	0.71	0.38	16.53	5.5	152
11	UnB	Axial 10.25/1	76.6	34	4.8	23.4	22.1	0.74	0.23	8.06	10	107
12	UnB	Axial 10.25/1	76.6	34	4.3	33.0	11.0	1.44	0.45	17.33	28.4	75
13	UnB	Axial 10.25/1	76.6	51	3.4	20.0	24.0	2.33	0.78	30.12	25	65
14	UnB	SH 1/6+2/10	157.6	34	5.4	36.0	13.0	1.66	0.32	33.8	1	-
15	UnB	Axial 10.25/1	177.6	34	3.8	34.8	13.7	2.70	0.36	38.52	18	52
16	ULB	HC	102.5	30	2.4	18.5	27.7	0.55	0.14	22.66	1	-
17	ULB	HC	102.5	30	2.5	19.6	26.7	0.54	0.15	22.62	1.1	-
18	ULB	PSW	102.5	30	5.1	18.1	29.2	0.36	0.11	25.66	1.5	-
19	ULB	PSW	102.5	30	5.4	20.8	33.1	0.35	0.11	25.37	3.8	-
20	ULB	SH 1.4/11	102.5	30	3.5	17.7	27.2	0.47	0.14	22.66	0.7	-
21	ULB	SH 1.4/11	102.5	30	2.5	16.5	30.0	0.54	0.14	23.44	1.2	-
22	ULB	SH 1.4/21	102.5	30	3.8	24.0	21.6	0.51	0.14	22.13	1.2	-
23	ULB	SH 1.4/21	102.5	30	4.1	25.3	28.4	0.43	0.12	24.9	1.2	-
24	ULB	SH 1.4/21	102.5	30	3.8	29.9	31.8	0.54	0.15	20.15	1.1	-
25	ULB	VOR	102.5	30	3.3	26.2	22.1	0.63	0.16	20.88	3.1	-
26	ULB	VOR	102.5	30	3.5	26.2	21.4	0.59	0.15	20.95	4.5	-
27	UnB	SH 1/6+2/10	56.6	34	13.9	38.5	6.5	0.89	1.17	23.19	6.4	118

A. Nature of Feed Coupled System Instability

From Table 3, it can be seen that the system was unstable for most of small injector pressure drop tests. As for the ULB campaign, injector pressure drops higher than 19 bar kept the system stable in all tests. These results are consistent with the stability limit analysis result in Section 3, except for tests #11, #13 and #14, from the UnB campaign. As mentioned earlier, it is clear that injector type has a great influence on combustion instability of hybrid rockets. However, this influence is much less important on the feed-system coupled instability under large pressure drop. It is expected that the injector geometry greatly influences other combustion instability modes, such as the intrinsic instability of hybrid rockets where the injection mass flow rate is decoupled from the chamber pressure [8-13].

The plots of the pressure for two hybrid engine tests conducted at UnB are shown in Fig. 7. The first plot is related to test #3 (showerhead injector), showing 19.1 bar of pressure drop and a very stable combustion. The second

plot refers to test #12 (one-hole axial injector) and presents severe pressure oscillations. Injectors with multiple small diameter orifices operate like a flow isolation element, decoupling the motor from the feed-system, thus blocking motor pressure disturbances propagation upstream through the oxidizer feed line. Oxidizer flow rate in motors with a large orifice injector (or without an injector) is strongly affected by the downstream pressure inside the combustor. Combustion instabilities related to feed-system mode may occur even in cases where a flow isolation element is used. Nevertheless, systems without a flow isolation element are much more prone to present instability [2, 7]. The showerhead injectors with multiple small diameter orifices could run as a flow isolation element, occurring flash vaporization phenomenon. Flashing of a two-phase flow system can attenuate pressure fluctuations traveling upstream through the oxidizer injector. Since nitrous oxide has a high vapor pressure liquid at room temperature, flash vaporization can occur within the injector orifice, making a two-phase flow. It was observed in [27] that mass flow rate approaches a critical value for injectors with large orifice length to diameter ratio (L/D), having flash vaporization, where the flow rate is independent of the downstream pressure. Thus, it might break the mechanism for coupling between the combustion chamber and the oxidizer feed system [27]. L/D of the one-hole injector is less than those of the showerhead injectors, as shown in Table 2. Therefore, it can be anticipated that, in the absence of other dumping effects, the one-hole injector has a strong tendency of propagating pressure waves to the oxidizer feed system. It can be seen that tests #11 and #13 (with the one-hole axial injector) generate large pressure oscillations, even though pressure drops above 22 bar, as shown in Table 3.

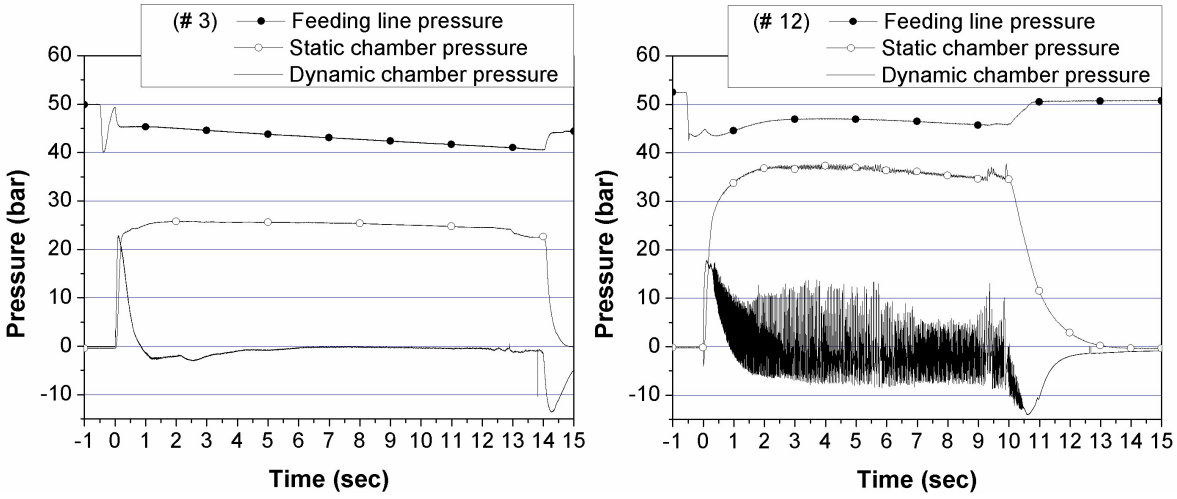

(a) (b)

Fig. 7 Chamber and feed pressure time traces for test #3(a) and #12(b): Injector type effect.

The influence of the pre-combustion chamber length on the stability of the system can be seen by comparing test #9 and test #14 with the relative longer pre-combustion chamber. The pre-combustion chamber length was 101 mm longer for the latter with respect to the former. Test #14 with the long pre-combustion chamber was very stable, even though it operated under relatively low injector pressure drop of 13 bar. The grain initial diameter and length, O/F ratio, the chamber pressure, and the injector pressure drop are equivalent or quite similar for both tests. Plots of system pressures, for both tests, are shown in Fig. 8. Considering that most of the parameters were analogous except for the pre-combustion chamber length, it was possible to conclude that the pre-combustion chamber design had a substantial influence on the pressure oscillations of the system. The long ~~large~~ pre-combustion chamber might have contributed to the stabilization of the system. From a practical point of view, however, such a long pre-combustion chamber length penalizes rocket weight and should be only considered after a trade-off analysis.

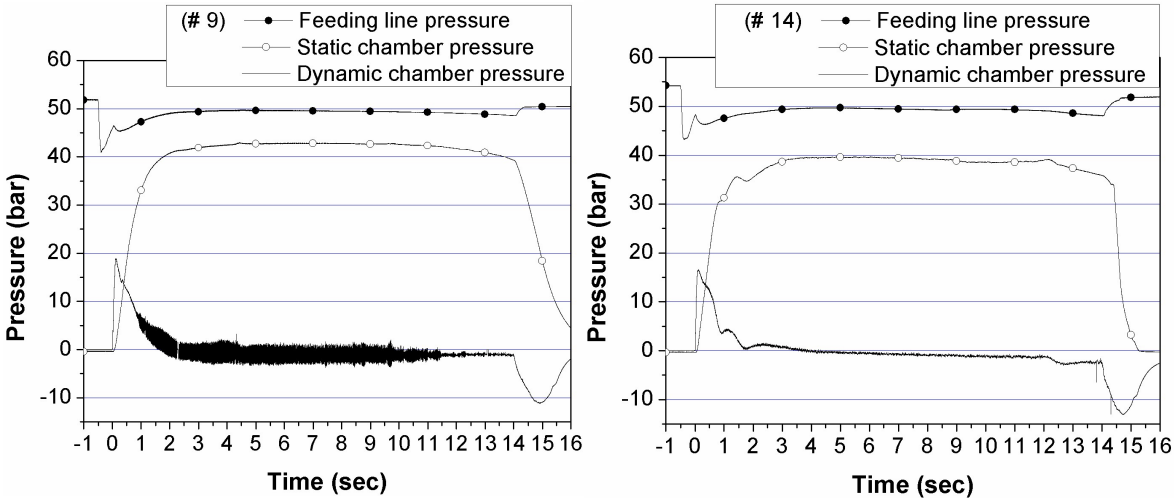

Fig. 8 Chamber and feed pressure time traces for #9(a) and #14(b); L_{pre} effect.

This result, a priori, may seem inconsistent with the result from the stability limit analysis in Section 3, from which reduced pre-combustion chamber length (or small τ_{pre}) is expected to improve the system stability. However, the relative role of the increased chamber volume, captured in θ_g parameter, should be considered in the analysis. From Eq. (11), τ_{pre} correlates linearly with pre-combustion chamber length while θ_g correlates with the total volume of the combustor. An increase in τ_{pre} due to a longer pre-combustion chamber is followed by an increase in the gas residence time inside the motor (θ_g). As it can be seen from Fig. 1, large θ_g increases the stability locus. Comparing

the parameters, test #14 had larger θ_g than test #9 thus favoring combustion stability. Nevertheless, it is not sufficient to investigate the stability behavior for test #14 only under the aspect of the θ_g increment, because the ratios between θ_g and τ_{pre} for tests #9 and #14 were similar and around 30. This is supposedly due to the fact that the role of ω^*_{comb} is important on the instability amplitude.

Figure 9 shows the stability limit curves for two values of ω^*_{comb} using the linearized model in Section 3 and the experimental data from the both test campaigns. The stable test cases #1 and #4 in which ΔP^* was larger than 4 were not plotted. It was confirmed from the stability limit analysis that the parameters such as the ratio of the injector pressure drop to the operating chamber pressure (ΔP^*), the pre-combustion chamber residence time (τ_{pre}), the gas residence time (θ_g), and the combustion time lag (τ_{comb}) strongly affect the stable region. The tests were not sufficient to investigate all the parameters in the model. Nonetheless, the proposed method could reasonably predict stability behavior of the system, although a detailed investigation on the influence of the parameter ω^*_{comb} on stability limits is needed to completely validate the model.

The tests from ULB had relatively large ΔP^* and θ_g/τ_{pre} which were sufficient to stabilize the combustion process. As shown in Fig. 9, ΔP^* higher than unity was a key factor for stable operation, except for tests #11 and #13, in which the one-hole injector was used. Tests #11 and #13, from the ΔP^* point of view, would fall in the stable region, based strictly on the theoretical analysis (Fig. 9). This type of injector design led to unstable operation regardless of the device`s pressure drop, as mentioned earlier. The level of pressure decay imposed by the injector of the order of 24 bar in test #13 was not sufficient to damp the pressure oscillations from the combustion chamber to the feed line, whereas the showerhead injector was able to decouple the pressure disturbances between the combustion chamber and the feed system at even lower pressure drop. Hybrid rocket engines without a flow isolation element are much more prone to feed-system coupled instability. The proposed linear system theory method cannot straightforwardly be applied to systems without some sort of isolation element.

Of great interest to the stability limit analysis is the smooth operation of test #14 which had the long pre-combustion chamber. Test #14 was conducted under stable conditions, whereas other tests, including test #9, with similar θ_g/τ_{pre} and ΔP^* to those of test #14 were unstable, as shown in Fig. 9. From the stability analysis applying the linearized model, it was possible to show that the stability limit curves are greatly influenced by ΔP^*, θ_g/τ_{pre}, and

ω^*_{comb} . Despite the similarities of ΔP^* and θ_g/τ_{pre} calculated for tests #14 and #9, respectively, the product $\omega \cdot \tau_{comb}$ (ω^*_{comb}) can be different for the tests #14 and #9. The parameter ω^*_{comb} depends on pre-combustion chamber length through ω which varies with the length. It has been observed that this is indeed case with long pre-combustion chamber length in Table 3, which is attributed to the fact that there is lower system frequency. The value of ω for #14 was around 500 rad/s, while the value for #9 was 840 rad/s. The range of ω for the other unstable test data, having the short pre-combustion chamber and the shower head injector, was 880 to 1040 rad/s. The parameter τ_{comb} was likely also to be altered as the pre-combustion chamber length increased. The incoming oxidizer in a long pre-combustion chamber has sufficient time to vaporize, as opposed to a short one. Thus, properties of the N_2O flow at the flame front, such as oxidizer temperature and vapor quality (m_{vapor}/m_{total}), depend on the pre-combustion chamber length. The properties influence τ_{comb}, and the coefficient c' might differ depending on pre-combustion chamber lengths. The stability limit curves for two arbitrary values of ω^*_{comb} are plotted in Fig. 9, and the parameter ω^*_{comb} might have influenced the stability behavior for #14. However, the investigation of the effect of ω^*_{comb} on the oscillation amplitude for #14 is not sufficient because of the difficulty in the calculation of the coefficient c' in the τ_{comb} model. c' should be estimated for specific operating conditions, and it can be different for each test, especially for different pre-combustion chamber lengths. However, it couldn't find out c' determined empirically in the scope of this research, and c' was assumed as 1.0 equally for the all tests.

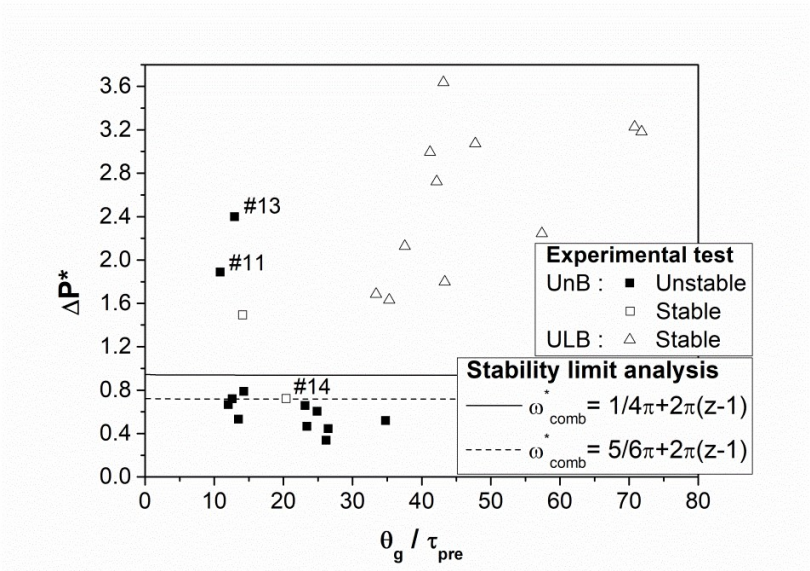

Fig. 9 Comparison of stability limit analysis for test data.

B. Feed Coupled System Instability Frequency Analysis

Figure 10 shows the chamber dynamic pressure plots and the Fourier Transform from test #9. From Table 3, it can be seen that the motor operated with the showerhead injector, 56.6 mm pre-combustion chamber length, and 34 mm initial fuel port diameter burning with an oxidizer to fuel ratio of 5.1. The combustion process took place at the initial chamber pressure of 37 bar with a pressure drop of 11.2 bar. The main operating parameters of the motor were: 0.64 ms for the pre-combustion chamber residence time; 0.34 ms for the combustion lag time; 23.59 ms for the gas residence time; and 133 Hz initial fundamental frequency from the short-time Fourier Transform result. The chamber pressure oscillated, around 6% of the mean chamber pressure, in a coherent fashion, and the instability characteristics resembles, to some extent, those from liquid rocket feed-system coupled instability. In liquid rocket engines, the feed system coupled instabilities are characterized by regular pressure oscillations, fairly uniform oscillations amplitude, reasonably narrow bandwidth peak of the Fourier Transform of the pressure signal, and a non-shift in time of the oscillation frequency, whereas Fig. 10 shows a wide range of oscillation frequencies which is typical of the hybrid rocket system dynamic pressure. The Fourier Transform indicated the fundamental frequencies spanning from about 50 to 140 Hz, which differs from liquid rocket engines, since pressure signals in liquid engines occur in narrow bandwidth. In hybrid rocket engines, the chamber volume changes as the fuel is consumed as opposed to the constant volume of liquid rocket engines. This change in volume occurred at the head and aft ends of the fuel grain as well as in the fuel port. The alteration of the volume of the pre-combustion chamber might have influenced on the instability frequency.

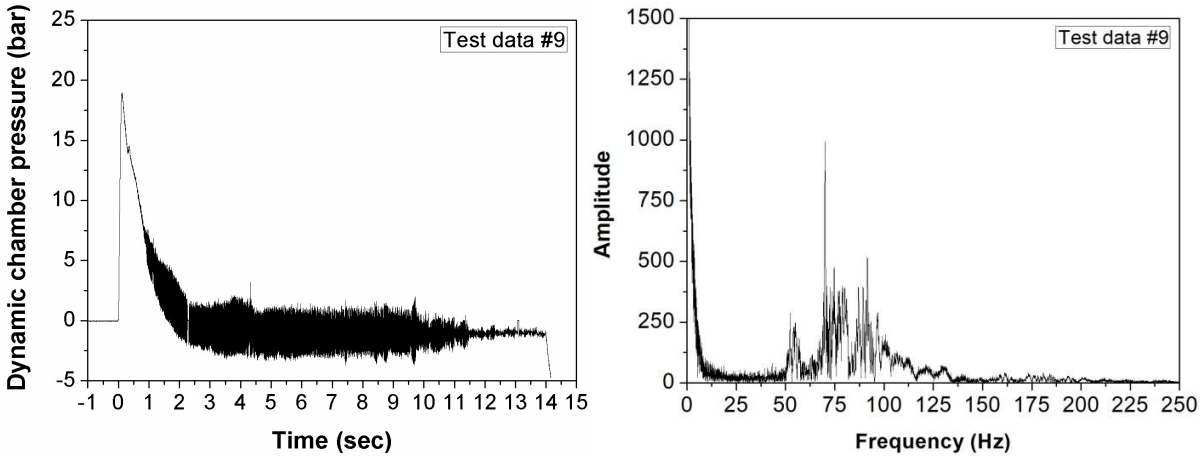

(a) (b)

Fig. 10 Chamber dynamic pressure time traces(a) and Fourier Transform(b) for test # 9.

The dynamic influence of the fundamental frequency of the combustion chamber can be analyzed in Fig. 11, where the frequency responses for the pressure signals obtained from tests #9 and #27 are shown. Both tests were conducted using the same motor configuration, except for the solid fuel types. Paraffin was used in test #9 while HDPE was used in test #27. The fundamental oscillation frequency does not shift significantly over time when HDPE was used as a solid fuel. Conversely, a shift in the fundamental frequency was observed for the burning of paraffin. An almost steady decay of the fundamental frequency over time, from 140 to 50 Hz, can be seen from the left plot in Fig. 11. In the tests, the fuel regression rate at the head end of solid grain was much higher for the paraffin than for the polymer fuel (HDPE), and the alteration in the pre-combustion chamber length was larger for test #9 than for test # 27. Therefore, one can infer that the pre-combustion chamber length has a strong influence on the fundamental frequency of the system.

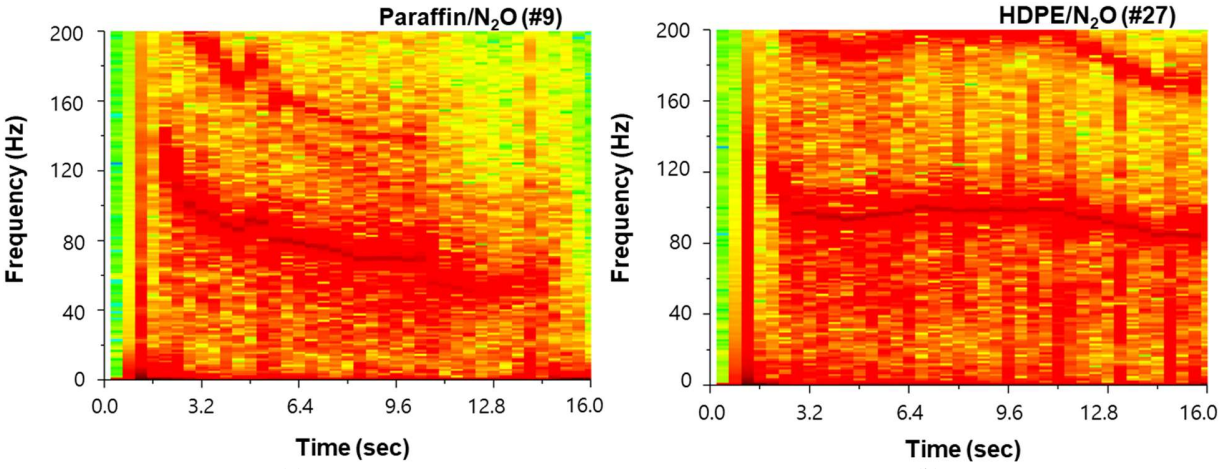

(a) (b)

Fig. 11 Contour plots of Fourier Transform in time-frequency for test #9(a) and #27(b).

A plot of the pre-combustion chamber residence times against the pressure oscillation frequencies indicates how the fundamental frequency correlates with τ_{pre}. Fig. 12 shows the fundamental frequency with respect to the pre-combustion chamber residence time (τ_{pre}) as calculated by the model, Eq. (11), for each test. It can be seen that the measured frequencies decrease as τ_{pre} increases, and the trend was also captured by the parametric analysis from Section 3.2. Therefore, one can infer that the pre-combustion chamber length and the flow velocity in a pre-

combustion chamber play a relevant role to the frequency response of the feed-system coupled instability in hybrid rocket engines.

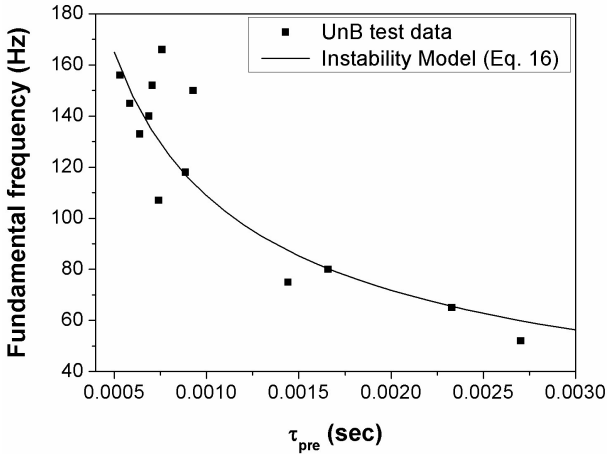

Fig. 12 Curve fit for feed-system coupled instabilities from UnB test data.

The correlation calculated from Fig. 12 gives the following equation for the fundamental frequency as a function of the pre-combustion chamber residence time.

$$f = \frac{1.73}{\tau_{pre}^{0.6}} = 1.73\left(u_{pre} / L_{pre}\right)^{0.6} \tag{16}$$

The constant, 1.73, in Eq. (16) depends on the operating conditions of a given hybrid rocket engine such as the quality parameter (χ). In this research, the nitrous oxide passed through the injector was assumed to be a mixture of 50% liquid and 50% gaseous N_2O.

VI.Conclusion

In this paper, feed-system coupled instabilities for hybrid rockets have been analyzed, both theoretically and experimentally. An extended mathematical model for the instability related to the coupling between the combustion chamber and feed system was developed, and experimental tests with significant combustion pressure oscillations were used to validate the model. The natures of the feed-system coupled instabilities for hybrid rocket engines were investigated, and the frequency analysis for the instability was performed.

The stability analysis based on the proposed extended model with typical linear dynamical system tools could be an effective method to predict the condition of stable and unstable regimes in typical hybrid motor configuration. The analysis confirmed that parameters such as the ratio of injector pressure drop to operating chamber pressure (ΔP^*), the ~~bulk~~ gas residence time (θ_g), the pre-combustion chamber residence time (τ_{pre}), and the combustion time lag (τ_{comb}) affect the pressure oscillation amplitude and the frequency of the feed system coupled instabilities for hybrid rockets.

Large injector pressure drop suppressed the feed system coupled instabilities, and ΔP^* higher than unity was a key factor for stable operation. The injector design is also a key element for the stability of the system, however this influence is much less important on the feed-system coupled instability under large pressure drop. Hybrid rocket engines without a conventional injector are much more prone to cause feed-system coupled instability. The long pre-combustion chamber contributed to the stabilization of the system, possibly due to ω^*_{comb} effect on the instability. The influence of ω^*_{comb} is significant on the oscillation amplitude for the feed system coupled instabilities, whereas τ_{comb} had a small effect on the oscillation frequency. More investigation on the influence of the parameter ω^*_{comb} on stability limits is needed to completely validate the model.

τ_{pre} significantly contributes to the period of the pressure oscillations. The pre-combustion chamber length and the flow velocity in a pre-combustion chamber play an important role in the frequency response of the feed-system coupled instability in hybrid rocket engines. The correlation $f=1.73/(\tau_{pre})^{0.6}$ was proposed in order to predict the instability fundamental frequencies. In spite of some similarities related to the feed-system response to pressure oscillation inside the combustor, hybrid rocket engines show a shift in the system frequencies over time, a particular characteristic not observed in liquid rocket engines.

References

[1] Sutton, G. P. and Biblarz, O., *Rocket Propulsion Elements,* 7th ed., John Wiley & Sons, Inc., New York, 2000.

[2] Karabeyoglu, A., "Combustion Instability and Transient Behavior in Hybrid Rocket Motors," *Fundamentals of Hybrid Rocket Combustion and Propulsion*, edited by M. J. Chiaverini, and K. K. Kuo, Vol. 218, Progress in Astronautics and Aeronautics, AIAA, Reston, VA, 2007, pp. 351–406.
doi:10.2514/4.866876

[3] Karabeyoglu, A., Zilliac, G., Cantwell, B. J., De Zilwa, S., and Castellucci, P., "Scale-Up Tests of High Regression Rate Paraffin-Based Hybrid Rocket Fuels," *Journal of Propulsion and Power*, Vol. 20, No. 6, 2004, pp. 1037–1045.
doi:10.2514/1.3340

[4] Fraters, A. and Cervone, A., "Experimental Characterization of Combustion Instabilities in High-Mass-Flux Hybrid Rocket Engines," *Journal of Propulsion and Power*, Vol. 32, No. 4, 2016, pp. 958-966.
doi: 10.2514/1.B35485

[5] Park, K. S., and Lee, C., "Low Frequency Instability in Laboratory-Scale Hybrid Rocket Motors," *Aerospace Science and Technology*, Vol. 42, April–May 2015, pp. 148–157.
doi:10.1016/j.ast.2015.01.013

[6] Greiner, B. and Frederick, R. A., Jr., "Experimental Investigation of Labscale Hybrid Instability," *30th Joint Propulsion Conference and Exhibit*, AIAA Paper 1994-2878, June 1994.
doi: 10.2514/6.1994-2878

[7] Guthrie, D. M. and Wolf, R. S., "Non-Acoustic Combustion Instability in Hybrid Rocket Motors," Report by American Rocket Company, Camarilla, CA, 1990.

[8] Boardman, T. A., Brinton, D. H., Carpenter, R. L., and Zoladz, T. F., "An Experimental Investigation of Pressure Oscillations and Their Suppression in Subscale Hybrid Rocket Motors," *31st Joint Propulsion Conference and Exhibit*, AIAA Paper 1995-2689, July 1995.
doi: 10.2514/6.1995-2689

[9] Boardman, T. A., Carpenter, R. L., and Claflin, S. E., "A Comparative Study of the Effects of Liquid-versus Gaseous-Oxygen Injection on Combustion Stability in 11-inch-Diameter Hybrid Motors," *33rd Joint Propulsion Conference and Exhibit*, AIAA Paper 1997-2936, July 1997.
doi: 10.2514/6.1997-2936

[10] Pucci, J. M., "The Effects of Swirl Injector Design on Hybrid Flame-Holding Combustion Instability," *38th AIAA/ASME/SAE/ASEE Joint Propulsion Conference & Exhibit*, AIAA Paper 2002-3578, July 2002.
doi: 10.2514/6.2002-3578

[11] Carmicino, C., "Acoustics, Vortex Shedding, and Low-Frequency Dynamics Interaction in an Unstable Hybrid Rocket," *Journal of Propulsion and Power*, Vol. 25, No. 6, 2009, pp. 1322-1335.
doi: 10.2514/1.42869

[12] Bellomo, N., Barato, F., Faenza, M., Lazzarin, M., Bettella, A., and Pavarin, D., "Numerical and Experimental Investigation of Unidirectional Vortex Injection in Hybrid Rocket Engines," *Journal of Propulsion and Power*, Vol. 29, No. 5, 2013, pp. 1097–1113.

doi: 10.2514/1.B34506

[13] Kim, J. and Lee, C., “Transition of Combustion Instability in Hybrid Rocket by Swirl Injection,” *ACTA ASTRONAUTICA*, Vol. 158, May 2019, pp. 323-333.
doi: 10.1016/j.actaastro.2018.07.036

[14] Crocco, L., and Cheng, S., *Theory of Combustion Instability in Liquid Propellant Rocket Motors*, Butterworths Scientific, London, 1956.

[15] Yang, V. and Anderson, W. E., *Liquid Rocket Engine Combustion Instability*, American Institute of Aeronautics and Astronautics, Inc., Washington. 1995.
doi: 10.2514/4.866371

[16] Summerfield, M., "A Theory of Unstable Combustion in Liquid Propellant Rocket Systems," *Journal of the American Rocket Society*, Vol. 21, No. 5, 1951, pp. 108-114.
doi: 10.2514/8.4374

[17] Casiano, M. J., “Extensions to the Time Lag Models for Practical Application to Rocket Engine Stability Design”, Ph. D. Dissertation, Mechanical Engineering, The Pennsylvania State University, University Park. PA., August 2010.

[18] Morita, T., Kitagawa, K., Yuasa, S., Yamaguchi, S., and Shimada, T., “Low-Frequency Combustion Instability Induced by the Combustion Time Lag of Liquid Oxidizer in Hybrid Rocket Motors,” *Japan Society for Aeronautical and Space Sciences and ISTS*, Vol. 10, No. ists28, 2012, pp. 37-41.
doi: 10.2322/tastj.10.Pa_37

[19] Kim, S., Moon, H., Kim, J., and Cho, J., “Evaluation of Paraffin–Polyethylene Blends as Novel Solid Fuel for Hybrid Rockets,” *Journal of Propulsion and Power*, Vol. 31, No. 6, 2015, pp. 1750-1760.
doi: 10.2514/1.B35565

[20] Lee, J., Kim, S., Moon, H., and Kim, J., “Mass Transfer Number Sensitivity on the Fuel Burning Rate in Hybrid Rockets,” *Journal of Propulsion and Power*, Vol. 31, No. 4, 2015, pp. 1041-1050.
doi: 10.2514/1.B35449

[21] Szuch, J. R., “Digital computer program for analysis of chugging instabilities,” NASA TN D-7026, 1970

[22] Karabeyoglu, M. A., De Zilwa, S., Cantwell, B., and Zilliac, G., “Modeling of Hybrid Rocket Low Frequency Instabilities,” *Journal of Propulsion and Power*, Vol. 21, No. 6, 2005, pp. 1107-1116.
doi: 10.2514/1.7792

[23] Harrje, D. T., *Liquid Propellant Rocket Combustion Instability*, NASA SP-194, Washington, D.C., 1972.

[24] Andrianov, A., Shynkarenko, O., Bertoldi, A. E. M., Barcelos, M. N. D., Jr., and Veras, C. A. G., "Concept and Design of the Hybrid Test-motor for Development of a Propulsive Decelerator of SARA Reentry Capsule," *51st AIAA/SAE/ASEE Joint Propulsion Conference*, AIAA Paper 2015-3941, July 2015.
doi: 10.2514/6.2015-3941

[25] Bouziane, M., Betoldi, A. E. M., Milova, P., Hendrick, P., and Lefebvre, M., "Development and testing of a Lab-Scale Test-Bench for Hybrid Rocket Motors," *2018 SpaceOps Conferences*, AIAA Paper 2018-2722, Marseille, France, May-June 2018
doi: 10.2514/6.2018-2722

[26] Bouziane, M., Bertoldi, A. E. M., Lee, D., Milova, P., Hendrick, P., and Lefebvre, M., "Design and Experimental Evaluation of Liquid Oxidizer Injection System for Hybrid Rocket Motors," *7th European Conference for Aeronautics and Space Sciences*, EUCASS2017-133, 2017.
doi: 10.13009/EUCASS2017-133

[27] Waxman, B. S., Cantwell, B., Zilliac, G., and Zimmerman, J. E., "Mass Flow Rate and Isolation Characteristics of Injectors for Use with Self-Pressurizing Oxidizers in Hybrid Rockets," *49th AIAA/ASME/SAE/ASEE Joint Propulsion Conference*, AIAA Paper 2013-3636, July 2013.
doi: 10.2514/6.2013-3636